The Journal of Physical Chemistry A

VOLUME 103, NUMBER 41, OCTOBER 14, 1999

FEATURE ARTICLE

OH Radical Formation from the Gas-Phase Reaction of Ozone with Terminal Alkenes and the Relationship between Structure and Mechanism

Suzanne E. Paulson,* Myeong Y. Chung, and Alam S. Hasson

Department of Atmospheric Science, University of California at Los Angeles,
Los Angeles, California 90095-1565

Received: June 17, 1999; In Final Form: August 23, 1999

The reactions of ozone with alkenes have been shown recently to lead to the direct production of OH radicals in quantities that vary from 7 to 100% depending on the structure of the alkene. OH radicals are the most important oxidizing species in the lower atmosphere, and the OH−alkene reaction is a large source of new OH radicals, important in urban and rural air during both day and night. Evidence for OH formation comes both from low-pressure direct measurements and from tracer experiments at high pressure. With the goal of measuring OH formation yields with good precision, a small-ratio relative rate technique was developed. This method uses small amounts of fast-reacting aromatics and aliphatic ethers to trace OH formation yields. Here, we report OH formation yields for a series of terminal alkenes reacting with ozone. Measured OH yields were 0.29 ± 0.05, 0.24 ± 0.05, 0.18 ± 0.04, and 0.10 ± 0.03 for 1-butene, 1-pentene, 1-hexene, and 1-octene, respectively. For the methyl-substituted terminal alkenes methyl propene and 2-methyl-1-butene, OH yields were 0.72 ± 0.12 and 0.67 ± 0.12, respectively. The results are discussed both in terms of their atmospheric implications and the relationship between structure and OH formation.

Introduction

Urban air contains a complex mixture of aliphatic, aromatic, and unsaturated compounds that depends strongly on local anthropogenic activities. The unsaturated compounds are typically dominated by terminal alkenes,[1−3] both because they are a component of combustion emissions[4] and because they react more slowly with OH and O_3 than do internal alkenes. For example, concentrations of the straight and branched chain terminal alkenes together account for 70% of the total alkenes, and 8% of the total VOC's in the EPA's 29 city 6−9 AM average ambient speciated hydrocarbon mixture.[5] For a total ambient hydrocarbon loading of 1 ppmC using the same data set, 1-butene, 1-pentene, methylpropene, and 2-methyl-1-butene average 7, 4, 9, and 4 ppbC, respectively.

Reaction with ozone is one of three major loss pathways for unsaturated compounds once they are released into the atmosphere. Alkenes react rapidly with the hydroxyl radical, and some very rapidly with the NO_3 radical. Reaction with ozone ranges from a few percent to the dominant loss pathway, depending on the structure of the alkene and local conditions. The reactions of ozone with alkenes in the gas phase produce a complex set of stable and radical products (for example, see ref 6). Several recent studies have provided evidence that these reactions lead to the direct production of OH radicals in variable quantities depending on the alkene.[7−12] Organic peroxy radicals (RO_2) are likely to accompany the production of OH,[7,13] and in many polluted conditions, RO_2 radicals quickly generate OH radicals via reaction with NO. OH and RO_2 radical formation from these reactions has a significant impact on the atmospheric chemistry of urban and rural air. In those regions of the

---

* To whom correspondence should be addressed.

10.1021/jp991995e CCC: $18.00

atmosphere with moderate alkene concentrations (a few hundred ppt or more), OH and RO_2 formation from O_3−alkene reactions is a major, and sometimes dominant, component of primary HO_x production (HO_x = OH, HO_2, and RO_2) during both day and night.[14,15] In air that is heavily influenced by anthropogenic emissions, the majority of this HO_x comes from trace quantities of alkenes with internal double bonds even though these compounds have very low concentrations.[14] In rural continental air, the major alkene contributors are isoprene and α-pinene, but contributions from trace quantities of other terpenes with internal double bonds can also be significant.[14] In many models of atmospheric chemistry, ozone−alkene reactions are still parametrized predominantly as radical sinks, reflecting the state of the understanding of these reactions that persisted until the early 1990s. In this paradigm, ozone is consumed by the initial reaction and production of any type of HO_x radical, including OH, HO_2, or RO_2, was small.[16−18]

Observations of OH and other radicals from ozone−alkene reactions was suggested as early as 1958.[19] Chemiluminescence studies indicated radical production,[20,21] including OH,[22,23] although the possibility that OH arose from the reaction of HO_2 with O_3 was difficult to rule out. The first suggestion of a peroxide rearrangement pathway for a carbonyl oxide was made in 1981 by Martinez, Herron, and Huie.[24] In 1987, Niki et al.[7] proposed this mechanism as a pathway to OH formation, which they used to explain the observed excess loss of alkene relative to O_3 in a study of 2,3-dimethyl-2-butene ozonolysis. In the early 1990s, Paulson et al.[25] and Atkinson et al.[8] carried this work further and showed that the OH formation varied widely with alkene structure and that for some alkenes the yield of OH is about unity, indicating that the OH formation pathway is the dominant reaction channel. These researchers used three methods to measure OH formation, two that can be applied to any alkene but carry high uncertainties (+50%, −33%[8], and >50%)[26] and another that can be applied to fast reacting alkenes and has a small uncertainty (∼±15%).[27] Recently, a few other groups have made measurements with other methods.[28−30] By now, agreement is good for some alkenes and marginal for others (Table 1).

Here, we report measurements of OH formation yields using the small-ratio relative-rate technique[31] for a series of straight-chain and methyl-substituted terminal alkenes shown in Figure 1. We also report the yield of propanal from 1-butene ozonolysis. Previous to this study, one OH formation yield has been reported for 1-butene, 1-pentene, 1-hexene, and 2-methyl-1-butene, and two each for methyl propene and 1-octene.

The OH formation pathway is interesting for two distinct reasons. First, it appears that it has large consequence in the formation of oxidants in urban and rural air where concentrations of alkenes exceeds a few parts per thousand. Second, because the pathway accounts for a large fraction of the reacted alkene, it provides a unique window into the rich chemistry of the carbonyl oxides that form in the gas phase. Here, we discuss first the general features of the mechanism, then our small-ratio relative-rate method of measuring OH yields. This is followed by a discussion of the evidence that OH is indeed formed in these reactions rather than a different oxidizing species, such as a thermalized carbonyl oxide. Next, we present the results of our experiments to measure the OH formation yield from the ozone reaction with six alkenes, and this is followed by a discussion of the mechanistic implications, relation of OH formation pathway to other possible pathways, and open questions. Finally, a brief section explores the atmospheric implications of OH, RO_2, and HO_2 formation from O_3−alkene reactions.

OH Formation

The mechanism of ozone reacting with alkenes was first suggested by R. Criegee in the late 1940s[32,33] and has been largely vindicated. Ozone adds across the double bond to form a primary ozonide, which decomposes to form vibrationally excited carbonyl oxide and carbonyl products (R1a−c for 1-butene). Some alkenes also exhibit an additional minor

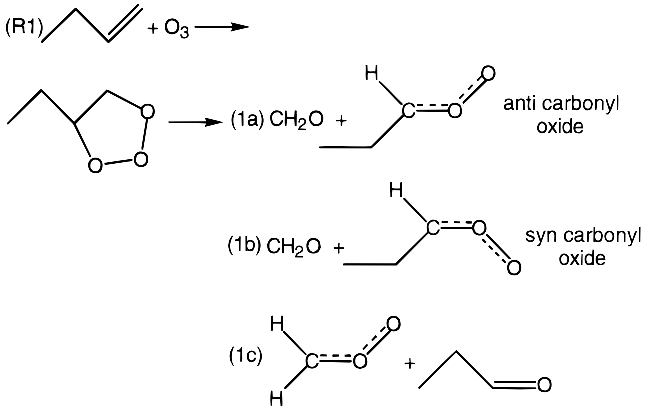

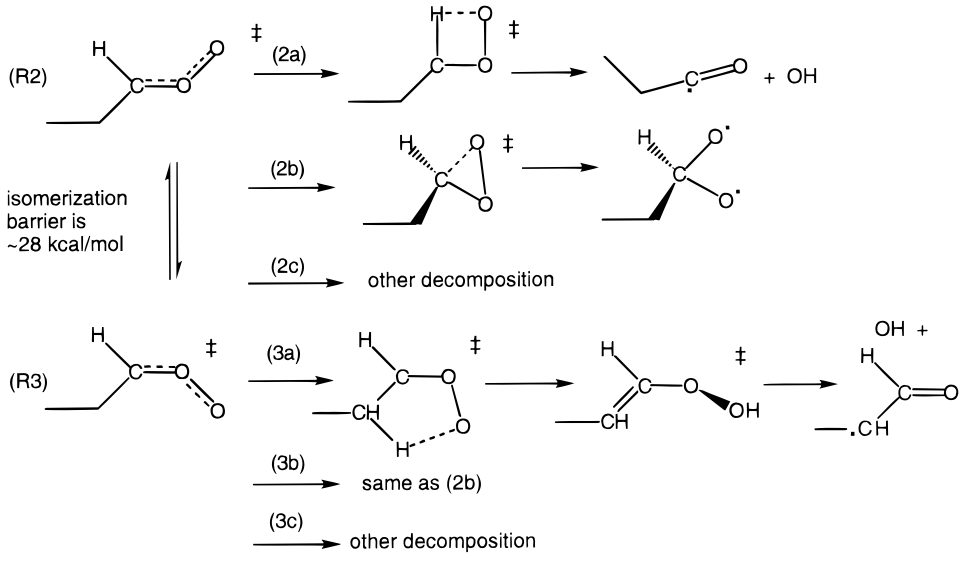

TABLE 1: Summary of OH Formation Yields

alkene	SRRRT^{a}	cyclohexane / cyclohexanol^{b}	butanol^{c}	other tracer^{d}	CO scavenger^{e}	"thermalized" carbonyl oxide yield^{f}
ethene	18 ± 6	12 (+6, −4)		14 ± 3	8 ± 1	39
propene	35 ± 7	33 (+16, −11)		32 ± 8	18 ± 2	25.4
1-butene	**29 ± 4**	41 (+20, −13)				
1-pentene	**24 ± 7**	37 (+19, −12)				
1-hexene	**18 ± 5**	32 (+17, −11)				
1-heptene		27 (+13, −8)				
1-octene	**10 ± 3**	18 (+9, −6)		45*		22 ± 11*
methyl propene	**72 ± 12**	84 (+42, −28)		60 ± 15		17.5
2-methyl-1-butene	**67 ± 12**	83 (+41, −27)				22^{g}
2,3 dimethyl-1-butene		50 (+25, −16)				
trans-2-butene	64	64 (+30, −20)		54 ± 13	24 ± 2	18.5
trans-2-pentene	47					
trans-3-hexene	47					
cis-2-butene	37	41 (+20, −13)		33 ± 8	17 ± 2	19^{d}
cis-2-pentene	30					
cis-3-hexene	36					
2-methyl-2-butene	100	89 (+44, −30)	93 ± 14	82 ± 16		10^{d}
2,3-dimethyl-2-butene	100	100 (+50, −33)	80 ± 12	70*, 89 ± 22		30^{g,}11d
1,3-butadiene	13 ± 3	8 (+4, −3)				
cyclopentene	62 ± 15	61 (+30, −20)				5.2
cyclohexene	54 ± 13	68 ((+34, −22)				3.2
cycloheptene	36 ± 8					2.9
1-methylcyclohexene	91 ± 20	90 (+45, −30)				10.4
1,2-dimethyl-cyclohexene		104 (+52, −34)	102 ± 16			
methylenecyclohexane	75					21.6
Styrene	7					26
α-methylstyrene	23					
trans-β-methylstyrene	22					
isoprene	25 ± 8	27 (+13, −9)		44 ± 11	19 ± 2	28^{d}
methylvinyl ketone	16 ± 5	16 ± 8				
methacrolein		20 (+10, −13)				
α-pinene	70 ± 17	83 (+41, −27)	76 ± 11	83 ± 21		12.5
β-pinene		35 (+17, −11)		24 ± 6		24.9
$\Delta^{3-\mathrm{carene}}$	100	106 (+53, −35)				
δ-limonene		86 (+43, −29)				
terpinolene		103 (+51, −34)				
β-phellandrene		14 (+7, −4)				
myrcene		115 (+58, −38)				
sabinene		26 (+13, −9)	33 ± 6			
ocimene (cis and trans)		63 (+31, −21)				
camphene		<18				
α-cedrene		67 (+33, −22)				
α-copaene		∼35				
β-caryophylene		6 (+3, −2)				
α-humulene		22 (+11, −7)				
cis-3-hexen-1-ol		0.26 (+13, −8)				
cis-3-hexenyl acetate		0.16 (+8, −5)				
trans-2-hexenal		∼0.62				
linalool		0.72				
2-methyl-3-butene-2-ol		19 (+9, −6)				

[a] Measurements made with the small-ratio relative-rate technique. Values without uncertainties are from unpublished work (Orzechowska et al.[73]) and should be considered preliminary. Bold indicates this work. Other values are published or in press[29,31,35], Fenske et al.[48] [b] Measurements by Atkinson, Aschmann, Arey and co-workers.[8,10,38,54,55,83] [c] Reference 27. [d] Reference 56, (*) except 2,3-dimethyl-2-butene, and 1-octene, which are from Niki et al.[7] and Paulson and Seinfeld, 1992,[26] respectively. These 1-octene values are only semiquantitative. Thermalized carbonyl oxide yields indicated with this superscript are from ref 56. [e] Reference 13. [f] Hatakeyama et al.[6] [g] 2,3-dimethyl-2-butene is from ref 7.

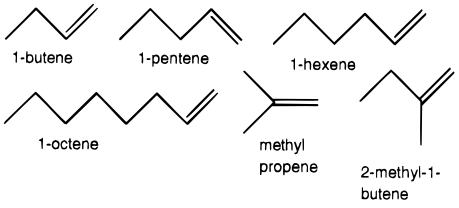

Figure 1. Alkene structures.

pathway (<5%) that generates an epoxide plus O_2.[34,35] Cycloreversion of the primary ozonide results in unequal branching (e.g., between R1a + R1b and R1c) for many alkenes. Grosjean and Grosjean,[36] Tuazon et al.,[37] and Atkinson et al.[38] have provided a large data set of aldehyde yields. In most cases, the aldehyde products are formed with 100% yield (within uncertainties).[36,39] In general, unbranched terminal alkenes show no preference for formaldehyde (R1a,b) over the substituted aldehyde (R1c). The one exception was 1-butene, with a literature branching ratio of about 65:35 HCHO:RCHO;[40] but below, we report a yield of propanal of 45%. Branched alkenes with a methyl (or other alkyl) group at the double bond show a preference for forming the less substituted aldehyde, presumably together with the more substituted carbonyl oxide; the HCHO:RCHO ratio is about 65:35 for methylpropene, 2-methyl-1-butene, 2-methyl-2-butene, 2,3-dimethyl-1-butene, and 2,3,3-trimethyl-1-butene.[36,37] β-pinene and camphene, both of which have exocyclic, unsubstituted double bonds, also display a preference for HCHO:RCHO formation greater than 50:50, although sabinene does not.[41] Compounds with a methyl group that is β to the double bond may have a slight preference for the substituted carbonyl oxide as well, but this pattern is less clear. Also, theoretical calculations predict preferences for formation of syn or anti carbonyl oxides from ozonolysis of symmetric internal alkenes and methyl-substituted double bonds, controlled by the primary ozonide cycloreversion transition states.[42,43]

While the subsequent chemistry of the carbonyl oxides in the liquid phase is fairly well understood,[44] the gas-phase still contains several puzzles and has been the subject of a rich literature spanning the intervening 5 decades. (R1) is exothermic by 50−60 kcal/mol (for example, see ref 45) so that the resulting carbonyl oxide and carbonyl products are vibrationally excited, the former sufficiently so to undergo unimolecular rearrangements and decomposition. The major pathways for the larger carbonyl oxides are illustrated in (R2−R3). A direct observation of the carbonyl oxide in the gas phase has yet to be made. Calculations indicate that the carbonyl bond exhibits a large fraction of double bond character and only a small amount of diradical character[46] resulting in a large syn−anti isomerization barrier, calculated at ∼35 and ∼28 kcal/mol.[47,48] This is a few kcal/mol lower than pathway R2a, estimated at ∼31 kcal/mol, but higher than formation of the dioxirane (R2b, R3b), ∼19 kcal/mol, and OH formation via the excited hydroperoxide intermediate (R3a) ∼14 kcal/mol;[45] the absolute values depend on the level of theory used to calculate the energies and the substituents about the double bond, but the ordering is now fairly well established.[13,47,48] The anti carbonyl oxide appears to be most likely to isomerize to the dioxirane (R2b); the next lowest path is isomerization to the syn carbonyl oxide. The lowest energy path for the nascent syn carbonyl oxide is to form OH (R3a); the next lowest energy path followed is isomerization to the dioxirane (R3b). Carbonyl oxides with two CH, CH_2, or CH_3 substituents clearly have abstractable hydrogen atoms for both possible conformers and should have high OH yields.

The C_1 carbonyl oxide may react as follows:

(R4)

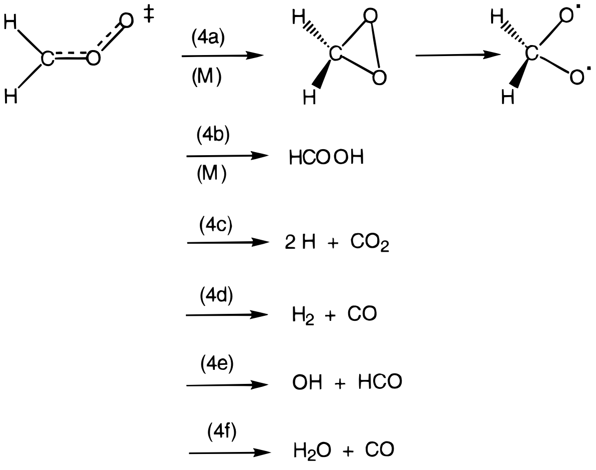

The C_1 carbonyl oxide may generate OH via a 1,3-hydrogen shift as shown in (R2a), but this pathway is predicted to be too inefficient to explain the observed value (about 18%, Table 1), ab initio/RRKM/master equations predict ∼0.5%,[49]although this is debated; see ref 12.

If syn carbonyl oxides are assumed to produce OH with unit yield and anti with nearly zero yield, then the number of possible syn and anti conformers determined by the substituents about the double bond provides a framework that is consistent with the OH yields that are observed. These follow in order: compounds with no available H for abstraction < terminal alkenes < internal alkenes < tri- and tetramethyl-substituted double bonds.[10] Within this framework, however, many additional subtleties exist.

The coproduct of OH formed through this mechanism is a substituted alkyl radical; in the atmosphere, this rapidly generates HO_2 in the presence of NO; HO_2 is then converted to additional OH in the atmosphere after reacting with NO, as shown in (R5). In the experiments described here, NO is not present so that

(R5)

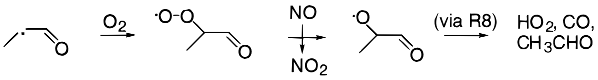

the RO_2 radicals formed in (R4) react with HO_2 or other RO_2 radicals to form organic peroxides, carbonyls, and alcohols.

$$RO_2 + HO_2\ (+M) \rightarrow ROOH\ (+M) + O_2 \qquad (R6)$$

$$RO_2 + RO_2 \rightarrow x ROH + x R{=}O + 2(1 - x) R{-}O^{\bullet} + (1 - x) O_2 \qquad (R7)$$

$$R{-}O^{\bullet}\ (+\ O_2) \rightarrow HO_2 + \text{other products} \qquad (R8)$$

The rate constants and branching ratios of (R6) and (R7) depend on the nature of the attached R group. In general, the R radical from the OH formation channel (R3) will produce some β-carbonyl-substituted $RO^{\bullet}$ radical via (R7), which may form HO_2 even in the absence of NO.

(R9a)

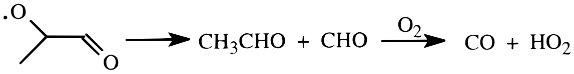

(R9b)

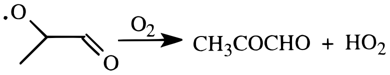

Experimental Methodology: Small-Ratio Relative-Rate Technique

Monitoring OH formation in ozonolysis reactions is confounded by the rapidity of alkene reactions compared to most other compounds. Alkenes react with OH at nearly gas-kinetic rates, most with rate constants in the range (2.6−36) × 10^{-11} cm^3 $molecule^{-1}$ s^{-1}. If the goal is to scavenge the majority of OH radicals (i.e., >95%) with the tracer, then the tracer must be added in large excess, 10 to 1000-fold depending on the tracer/alkene combination. A tracer can be any compound that reacts with OH but only slowly with O_3 (or HO_2 or other potential reaction partners).

$$O_3 + \text{alkene} \xrightarrow{k_{O_3}} y_{OH} OH + y_{OH} RO_2 + R_2C{=}O + x_1 HO_2 + x_2 \text{ “thermalized” Criegee intermediates} + \text{other products} \qquad (R10)$$

$$OH + \text{alkene} + M \xrightarrow{k_A} RO_2 + M \qquad (R11)$$

$$OH + \text{tracer} + M \xrightarrow{k_{tr}} RO_2 + M \qquad (R12)$$

Under these conditions, even if 100% of the alkene is reacted (and especially if the OH formation yield is significantly less than unity), only a small fraction of the tracer reacts. Deriving information from the amount of tracer reacted then carries a large uncertainty since it requires measuring small differences

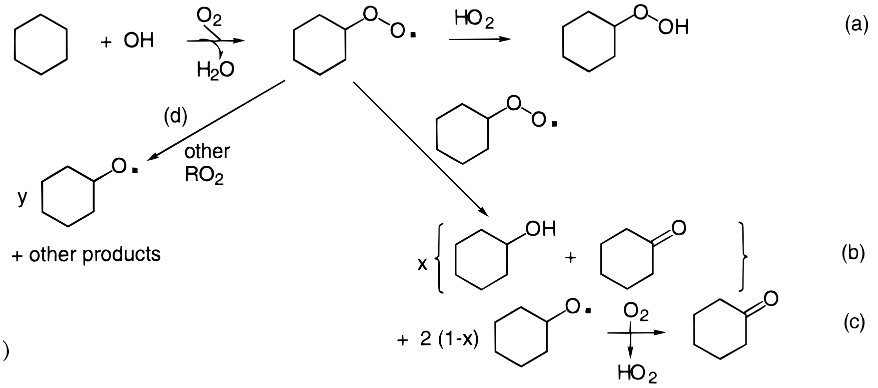

(R15)

between large numbers. However, when a small amount of tracer is added, a measurable percentage of the tracer reacts away, up to 40% depending on k_A, k_{Tr}, and yOH. This is the basis of the small-ratio relative-rate technique, which has been described in detail elsewhere.[31] The best tracers react rapidly with OH. 1,3,5-trimethylbenzene (TMB), *m*-xylene (XYL), di-*n*-butyl ether (DBE), and di-*n*-propyl ether are excellent choices. OH yields are most accurately calculated by numerically solving the equation set that describes the full chemistry of the reactants and products, as well as any minor inorganic sources of OH radicals such as the side reactions

$$H + O_3 \rightarrow OH + O_2 \qquad (R13)$$

$$HO_2 + O_3 \rightarrow OH + 2O_2 \qquad (R14)$$

Because the chemistry is dominated by (R10−12), a calculation of the OH yield using a simple analytical expression comes within about 20% of the numerical result; for a detailed discussion, see Paulson et al.[31] Because of the somewhat higher precision, experiments described here were analyzed numerically.

Evidence and Quantification of OH Formation

Five lines of experimental evidence indicate OH is formed in the ozonolysis of alkenes: (1) excess alkene consumption compared to O_3 consumption (indicating an additional loss process for the alkene[7,50]); (2) reaction of tracers that react with OH but only slowly with O_3 (e.g., see ref 25); (3) formation of products consistent with OH reactions with alkenes and tracers (e.g., see refs 8, 11, 13, 27); (4) recent studies monitoring relative consumption rates of pairs of tracers are consistent with OH reaction;[11,30] (5) most importantly, Donahue et al.[12] have recently observed the OH radical directly using laser-induced fluorescence (LIF) in low-pressure flow tube studies of ozone−alkene reactions. Further, Pfeiffer et al.[51] have observed OH directly from atmospheric pressure ozonolysis of terpenes using multicomponent optical absorption spectroscopy (MOAS). The OH formation mechanism involving a vibrationally excited hydroperoxide intermediate (R3a) has also recently been thermochemically described.[12,13,45,47]

The above methods have also been applied to quantify OH yields. A large, self-consistent data set has been developed by Atkinson and co-workers (Table 1) by monitoring products from reaction of cyclohexane with OH in O_3−alkene systems. OH reacts with cyclohexane to make a cyclohexylperoxy radical that partially disproportionates to cyclohexanone plus cyclohexanol (R15b). Cyclohexanone is also generated from cyclohexoxy radicals arising from the cyclohexylperoxy radical reactions with itself and other RO_2 radicals (R15c,d), and as such, the ratio of cyclohexanol to cyclohexanone from different alkenes varies.[8] The cyclohexylperoxy radicals can also react with HO_2 to form a hydroperoxide (R15a). Since the HO_2 concentration in the experiment is not known, the cyclohexane method carries an uncertainty estimated by Atkinson et al.[8] to be approximately −33% + 50%. Recently, Atkinson and co-workers have developed a method that provides OH yield measurements with higher accuracy, about ±15%.[27] This method measures formation of 2-butanone from the reaction of 2-butanol with OH, a reaction that does not involve an RO_2 intermediate. Because the 2-butanol contains small quantities of impurities that result in the formation of 2-butanone in the absence of alkenes, this method is best applied to alkenes that react rapidly with ozone (i.e., $k > 8 \times 10^{-17}$ cm^3 molec^{-1} s^{-1}).[27] Gutbrod et al.[13,28,45] have measured OH formation by adding CO in large excess and monitoring CO_2 formation. Tracer loss methods where the tracer is at equal or higher concentration than the alkene[25,52] and other methods generally have higher uncertainties, although moderate concentrations of tracers can provide reasonable results if the tracers are highly reactive.[53] Our small-ratio relative-rate measurements (described below) of OH formation monitor consumption of pairs of tracers as well, but because the initial amount of tracer is small, the tracer consumed can exceed 40% and results in uncertainties of ±15−30%. The LIF measurements carried out at 4−7 Torr by Donahue et al.[12] have estimated uncertainties of ∼±50%, and the MOAS measurements are semiquantitative. Measurements of OH yields by more than one method often agree within reported uncertainties, e.g., to within 50% (Table 1). The measurements made by Chew and Atkinson[27] with the butanol method, those made by our group, several of the measurements of by Atkinson et al. using the cyclohexane method,[8,10,38,54,55] and several of those by Rickard et al.[56] agree to within ±15%. The results from other methods are variable; the LIF measurements are generally higher, but again, they were made at low pressure, the CO measurements lower, and the cyclohexane method, if not in close agreement then higher. The reason that the yields measured with the CO method[28] are lower remains unclear, but see ref 57 for a possible explanation.

Schaefer et al.[52] suggested that the reactive species was not OH but another radical such as the carbonyl oxide itself. This suggestion was based on a comparison of the relative loss rates of pairs of tracers with that expected for OH reaction. For experiments where pairs of tracers are used, the well-known relative-rate analysis may be applied to "derive" OH rate constants for the tracers. In this analysis, the O_3 reaction with the alkene is simply the source of OH (or other) radicals, and the experiments are directly analogous to studies that use H_2O_2 or CH_3ONO as an OH source (e.g., see ref 58). The relative rate method is based on simultaneous monitoring of the tracer concentrations as they react.

$$\mathrm{OH} + \mathrm{tracer}_1 \xrightarrow{k_{\mathrm{Tr}_1}} \mathrm{products} \tag{R16}$$

$$\mathrm{OH} + \mathrm{tracer}_2 \xrightarrow{k_{\mathrm{Tr}_2}} \mathrm{products} \tag{R17}$$

The slope of a plot of the logs of the two tracer concentrations is equal to the ratio of the respective OH rate constants in the absence of other loss processes (e.g., see ref 59),

$$\frac{k_{\mathrm{Tr}_1}}{k_{\mathrm{Tr}_2}} = \frac{\ln([\mathrm{Tr}_1]_0/[\mathrm{Tr}_1]_t)}{\ln([\mathrm{Tr}_2]_0/[\mathrm{Tr}_2]_t)}$$

where k_{Tr_i} and Tr_i are the OH reaction rate constants and concentrations, respectively, for the *i*th tracer. Schaefer et al.[52] used this approach, but used slowly reacting alkane tracers in fairly large concentrations, and measured changes in the tracer concentrations of less than 5%. Our small-ratio relative-rate measurements of OH formation monitor consumption of pairs of tracers as well, but small amounts of more rapidly reacting alkyl aromatic and aliphatic ether are used such that the amount of tracer consumed in our experiments averaged 31, 14, and 16% for TMB, XYL, and DBE, respectively. To date, we have measured and calculated the ratio of consumption of pairs of tracers in 60 experiments using 16 alkenes and two tracer pairs: TMB/*m*-xylene (XYL) and TMB/di-*n*-butyl ether (DBE). Averages of 2.43 ± 0.09 and 2.01 ± 0.06 for $k_{\mathrm{TMB}}/k_{\mathrm{XYL}}$ and $k_{\mathrm{TMB}}/k_{\mathrm{DBE}}$, respectively, were measured ($2\sigma_{\mathrm{m}}$[11,29,43]). Here, we use σ_{m}, the standard deviation of the mean value, as a more stringent comparison between the expected and observed values.[60] The expected values of $k_{\mathrm{TMB}}/k_{\mathrm{XYL}}$ and $k_{\mathrm{TMB}}/k_{\mathrm{DBE}}$ for OH reaction based on the literature are 2.4 ± 1.0 and 2.0 ± 1.0.[58] We have measured the rate constants for the reactions of OH with TMB, XYL, and DBE in a separate study using the same analytical equipment and chambers, using methylnitrite photolysis as the OH source. Our measurements of the rate constants for TMB and DBE reacting with OH were nearly identical to the recommended literature values, and that for XYL reaction with OH is about 7% lower, giving $k_{\mathrm{TMB}}/k_{\mathrm{XYL}}$ and $k_{\mathrm{TMB}}/k_{\mathrm{DBE}}$ of 2.6 ± 0.11 and 1.98 ± 0.08 ($2\sigma_{\mathrm{m}}$), respectively.[61] The $k_{\mathrm{Tr1}}/k_{\mathrm{Tr2}}$ values from OH generated in ozone−alkene reactions are in excellent agreement (deviation is less than 3% in both cases) with the $k_{\mathrm{Tr}_1}/k_{\mathrm{Tr}_2}$ values for OH generated from a variety of different sources used in the studies reported in the literature.[11] For measurements in our lab, agreement is within 7%. Recently, Marston et al.[30] performed a similar study on 2-methyl-2-butene ozonolysis using eight different tracers including alkenes, alkanes, and aromatics. They found excellent consistency with OH in all but one case. In conclusion, the relative consumption of the two pairs of tracers is consistent with OH formation from the O_3 reaction with alkenes.

Our findings and those of Marston et al.[30] are not in agreement with the results of Schaefer et al.[52] The reason for this discrepancy is not entirely clear, but in their experiments, less than about 5% of the tracers reacted. Schaefer et al.[52] reported a precision of ∼±0.5%; however, this might be an underestimation given that the sample composition changes through the experiment. Along these lines, we observe that the variance in the slopes increases remarkably as the initial tracer/alkene ratio is increased and less tracer reacted; for 16 experiments where less than 20% of the initial TMB reacted, we had $k_{\mathrm{TMB}}/k_{\mathrm{XYL}}$ of 2.2 ± 0.4 and $k_{\mathrm{TMB}}/k_{\mathrm{DBE}}$ of 2.0 ± 0.5 ($2\sigma_{\mathrm{m}}$).

Thermalized Carbonyl Oxides

There are three candidates for the structure of the thermalized carbonyl oxides, the peroxy, bisoxy, and dioxirane forms (R2,R3), and little data to indicate which form is the one that can undergo secondary reactions. Calculations by Olzmann et al.[49] suggest that a portion of the initial carbonyl oxides from ethene may be formed cold, or thermalized, an idea that is consistent with the observation of Hatakeyama et al.[6] that the yield of thermalized carbonyl oxide from ethene does not go to zero at low pressures. Since the nascent carbonyl oxide is very likely a peroxy form, this suggests that the thermalized carbonyl oxides are also "peroxy." The observation of organic peroxide products from the reaction of thermalized carbonyl oxides with water and alcohols suggest reaction of the peroxy form as well.[62] Experimental evidence for the dioxirane comes from Mihelcic et al.[63] using matrix isolation electron spin resonance spectroscopy (ESR), who did not observe the dioxirane itself, but found no evidence for the radical electrons of the bisoxy or peroxymethylene products from ethene ozonolysis. Theoretical calculations indicate however that the carbonyl oxide (peroxymethylene) should not produce an ESR signal; it is a closed-shell species and has only about 5% diradical character.[46] It should be noted that the dioxirane has been observed as a product of ozonolysis,[64] although this does not require the thermalized carbonyl oxide to be the dioxirane. The observation of hydroxymethylformate from the CH_2OO−formaldehyde reaction,[65] which had provided credence to a dioxirane or bisoxy form of the thermalized carbonyl oxide, has recently been shown to be hydroperoxymethylformate instead.[66]

Experimental Description and Numerical Analysis

The experimental approach has been described in detail elsewhere[31] and is only briefly described here. Experiments were carried out at 296 ± 2 K in 200 ± 50 L Teflon chambers. The chambers were placed in a dark enclosure to eliminate any possible photochemistry. Hydrocarbons were evaporated (liquids) or injected (gasses) into a stream of purified air (Thermo Environmental model 111) as the chamber was filled. Purchased hydrocarbons (Aldrich) had stated purities of 98% or better and were used as received. Hydrocarbon concentrations were monitored throughout the experiments with a gas chromatograph/flame ionization detector (GC/FID) (Hewlett-Packard 5890), equipped with a 30 m × 1 μm film × 0.32 mm i.d. DB-1 column (J&W). The GC was calibrated daily with either a 20.2 ± 0.4 ppm *n*-hexane or 4.9 ± 0.1 ppm cyclohexane standard (Scott Specialty Gases). Calibration standards for TMB, DBE, 1-butene, 1-pentene, and 1-hexene (all certified to ±2%) were run periodically, and these responses, relative to hexane (or cyclohexane), were used to determine the concentrations of these compounds. For all other compounds, the number of carbon atoms was used to calculate the FID response normalized to the hexane (or cyclohexane) calibration. Ozone was generated in aliquots by flowing pure O_2 (at 100 S $\mathrm{cm}^3\ \mathrm{min}^{-1}$ for 30−90 s) through a mercury lamp generator (JeLight PS-3000-30) and was monitored with UV absorption (Dasibi 1003-RS).

The initial hydrocarbon concentrations were determined 30−60 min after filling the chamber. Next, a series of O_3 aliquots were added, each immediately following injection of a sample into the GC to allow maximum time for mixing and reaction before the next measurement. Experiments lasted 3−6 h and had average O_3 concentrations of 0.5 ppm or less. Because both the chemistry and the chromatogram become more complex as the experiment progresses, experiments were terminated once 55−75% of the initial alkene had reacted. Concentrations of alkenes and tracers were generally chosen such that $[\mathrm{Tr}]_0/[\mathrm{A}]_0 < 0.12$, and the tracer concentration was sufficiently large that it could be easily measured with GC/FID without preconcen-

TABLE 2: Summary of Initial Conditions for OH and Propanal Yield Experiments

alkene/tracer(s)	initial concentration(s) (ppm)			calculated OH yield(s)		
expt. no.	BX-73	BX-719	BX-721	BX-73	BX-719	BX-721
1-butene	9.59	9.95	11.4			
m-xylene	0.515	0.401	0.269	0.30	0.275	0.32
TMB	0.461	0.418	0.336	0.29	0.275	0.29
expt. no.	BT-921		BT-922	BT-921		BT-922
1-butene	12.8		6.95			
TMB	1.63		3.50	0.25		0.29
1-butene		average OH yield			0.29	
		st. dev. of mean ($2\sigma_m$)			0.02	
1-butene cyclohexane	6.24	8.34		(propanal yield experiments)		
	3500	3500				
expt. no.	PT-424	PT-91	PT-425	PT-424	PT-91	PT-425
1-pentene	6.09	5.19	8.13			
TMB	0.652	0.579	0.699	0.21	0.27	0.27
expt. no.	PX-84	PX-97	PX-811	PX-84	PX-97	PX-81
1-pentene	8.92	8.07	13.9			
m-xylene	0.480	0.635	0.391	0.23	0.23	0.305
TMB	0.460	0.591	0.338	0.22	0.19	0.24
expt. no.	PX-829			PX-829		
1-pentene	12.2					
XYL	0.742			0.27		
1-pentene		average OH yield			0.244	
		st. dev. of mean ($2\sigma_m$)			0.03	
expt. no.	HX-93	HX-94	HX-911	HX-93	HX-94	HX-911
1-hexene	10.7	11.4	9.78			
m-xylene	0.435	0.470	0.444	0.19	0.17	*a*
TMB	0.437	0.428	0.435	0.19	0.18	0.18
1-hexene		average OH yield			0.18	
		st. dev. (2σ)			0.02	
expt. no.	OX-226			OX-226		
1-octene	7.97					
XYL	0.16			*b*		
TMB	0.23			0.10		
expt. no.	OT-301			OT-301		
1-octene	6.05					
TMB	0.23			0.10		
1-octene		average OH yield			0.10	
expt. no.	Mp-301		Mp-302	Mp-301		Mp-302
methyl propene	6.20		6.16			
XYL	0.21		0.20	0.77		0.68
TMB	0.24		0.23	0.70		0.71
expt. no.	Mp-226			Mp-226		
methyl propene	5.97					
TMB	0.15			0.70		
methyl propene		average OH yield			0.70	
		st. dev. of mean ($2\sigma_m$)			0.03	
expt. no.	Mb-627	Mb-829		Mb-627	Mb-829	
2-methyl-1-butene	2.58	9.04				
m-xylene	0.267	0.539		0.71	0.67	
TMB	0.232	0.570		0.65	0.65	
expt. no.	Mb-428	Mb-430	Mb-55	Mb-428	Mb-430	Mb-55
2-methyl-1-butene	20.4	14.1	8.38			
TMB	1.40	0.453	0.576	0.73	0.65	0.61
2-methyl-1-butene		average OH yield			0.67	
		st. dev. of mean ($2\sigma_m$)			0.04	

[a] A product peak partly coeluted with the XYL peak during this experiment, making peak integration impossible. [b] The decrease in this tracer was too small to provide a reliable slope.

tration. Initial concentrations were for alkenes 2.5−21 ppmv and 0.2−3.5 ppmv for tracers (Table 2).

Experiments to determine the propanal formation yield from O_3 reacting with 1-butene were performed in a manner similar to those above, except that excess cyclohexane was used to scavenge more than 98% of the OH radicals. The FID response factor of two equivalent carbons was assumed, as per Jorgensen et al.,[67] a value that has been confirmed in our laboratory.[35,68,69]

The reaction sets used for numerical analysis of the OH yield experiments were developed from several sources. The rate constants for OH and O_3 reactions of alkenes and tracers are summarized in Table 3. Alkene-specific chemistry is described

TABLE 3: Summary of Rate Constants for Primary Reactions

compound	reaction partner	rate constant cm^3 $molec^{-1}$ s^{-1}	reference
1-butene	OH	3.14×10^{-11}	39
	O_3	9.64×10^{-18}	39
1-pentene	OH	3.14×10^{-11}	39
	O_3	1.0×10^{-17}	39
1-hexene	OH	3.7×10^{-11}	39
	O_3	1.1×10^{-17}	39
methylpropene	OH	5.14×10^{-11}	39
	O_3	1.13×10^{-17}	39
2-methyl-1-butene	OH	6.1×10^{-11}	39
	O_3	1.6×10^{-17}	39
1,3,5-trimethylbenzene	OH	5.73×10^{-11}	61
m-xylene	OH	2.2×10^{-11}	61
di-*n*-butyl ether	OH	2.89×10^{-11}	61

below. The OH radical is assumed to be co-generated with RO_2 radicals which react with rates that are comparable to β-hydroxy-RO_2 radicals, since they presumably have a β-carbonyl group, and are 1°, 2°, or 3° depending on the structure of the parent alkene. RO_2 chemistry is from Lightfoot et al.[70] The reactions of common products, RO_2 radicals, and tracers are listed in detail in ref 29. The primary products for O_3 and OH reactions with 1-butene, 1-pentene, and 1-hexene analogous to those of propene were assumed,[31] except that the carbonyl yields were adjusted according to Atkinson[39] and this work. Unreactive and slowly reacting products such as CO, CO_2, and H_2 are ignored. The only adjusted parameter was *y*, the yield of OH and 2°-β-hydroxyperoxy radicals. The (final) products assumed for the O_3 reactions with 1-butene through 1-octene were as follows:

$$\mathrm{RCH_2CH{=}CH_2} + \mathrm{O_3} \rightarrow 0.57\text{formaldehyde} + x\mathrm{RCH_2C(H){=}O} + 0.12\mathrm{HO_2} + y\,2°\text{-}\beta\text{-hydroxyperoxy radical} + y\mathrm{OH} \quad \text{(R18)}$$

R = CH_3, CH_3CH_2, $CH_3(CH_2)_2$, or $CH_3(CH_2)_4$, $x = 0.45$, 0.5, 0.52, or 0.5 (ref 39, this work), and $y = 0.29$, 0.24, 0.18, and 0.10 for 1-butene, 1-pentene, 1-hexene, and 1-octene, respectively.

Carbonyl products for ozone reactions with 2-methylpropene were an average of those from refs 36 and 37, and 2-methyl-1-butene carbonyl products were from Grosjean and Grosjean.[36]

$$\text{methyl propene} + \mathrm{O_3} \rightarrow 1.0\text{formaldehyde} + 0.31\text{acetone} + 0.12\mathrm{HO_2} + 0.72\ 2°\text{-}\beta\text{-hydroxyperoxy radical} + 0.72\mathrm{OH} \quad \text{(R19)}$$

$$\text{2-methyl-1-butene} + \mathrm{O_3} \rightarrow 0.66\text{formaldehyde} + 0.35\text{butanone} + 0.12\mathrm{HO_2} + 0.67\ 2°\text{-}\beta\text{-hydroxyperoxy radical} + 0.67\mathrm{OH} \quad \text{(R20)}$$

The calculated OH yields are most sensitive to the OH rate constants of the tracers. The yields are not particularly sensitive to the assumptions made about the products; a detailed investigation indicated that the uncertainty in the products introduces about ±5−6% uncertainty for propene.[31] Since all of the alkenes discussed here react with OH as or more rapidly than propene, reactions of OH with products are less important and the results are less sensitive to products, although at the same time, the products are more uncertain. These systematic uncertainties are combined into the total uncertainties reported below.

Results and Discussion

Representative data and calculations for the straight chain 1-alkenes are shown in Figure 2. The amount of tracer consumed depends primarily on a combination of the ratio k_{Tr}/k_A and the OH yield. Large OH−alkene rate constants and small OH yields both act to decrease the slope of these plots, and in all cases, the slope of the TMB curves is much higher than those of the more slowly reacting *m*-xylene and di-*n*-butyl ether. The 1-butene through 1-octene series has both moderate OH yields and OH reaction rate constants. The OH yields decrease with increasing size, and at the same time, the rate constants increase somewhat so that lower slopes are observed for the larger alkenes. The initial Tr/A ratios were varied somewhat, accounting for some of the scatter observed between runs with the same alkene.

The average calculated OH yield and 2σ uncertainties for O_3 reaction with 1-butene, 1-pentene, 1-hexene, and 1-octene are 0.29 ± 0.02, 0.24 ± 0.03, 0.18 ± 0.02, and 0.10 ± 0.02, respectively. These uncertainties reflect the random variability in the experimental data and need to be combined with the systematic uncertainty of about ±15% that arises from uncertainty in the OH rate constants, products, and so forth (above). Thus, the best estimates of the OH yields are 0.29 ± 0.05, 0.24 ± 0.05, 0.18 ± 0.04, and 0.10 ± 0.03.

Representative data for methylpropene and 2-methyl-1-butene are shown in Figure 3. The average calculated OH yield and combined 2σ random and systematic uncertainties for O_3 reaction with methyl propene and 2-methyl-1-butene are 0.72 ± 0.12 and 0.67 ± 0.12, respectively.

The OH formation yields from ozonolysis of the six terminal alkenes studied here have also been measured by Atkinson and co-workers using the cyclohexanone/cyclohexanol method (R15),[10,38] finding values for 1-butene, 1-pentene, 1-hexene, and 1-octene of 0.41, 0.37, 0.32, and 0.18, respectively, all with uncertainties of a factor of 1.5 (+50%, −33%).[10,38] A value for 1-octene of 0.45 ± 0.22 was also measured by Paulson and Seinfeld,[26] but this measurement, which monitored loss of a slowly reacting tracer (methylcyclohexane), is only semiquantitative. For methylpropene and 2-methyl-1-butene, Atkinson and Aschmann[10] measured OH yields of 0.84 and 0.83, again with uncertainties of a factor of 1.5. Within the mutual uncertainties, our measurements are in agreement with the results of Atkinson and co-workers[10,38] using the cyclohexane method, but in this case the difference in OH yields is a fairly consistent 8−14% OH per alkene reacted for the straight chain terminal alkenes and 20−25% for the branched terminal alkenes. This is in contrast to much closer agreement between the two laboratories for many other alkenes. Figure 4 compares OH yields for terminal alkenes measured by our laboratory (this work and ref 31) and by Atkinson and co-workers.[8,10,38] For the unbranched compounds, both data sets increase from ethene to propene and decrease from 1-butene onward as the carbon chain length increases. Since the method we used to measure the OH yields has a smaller uncertainty than the cyclohexane method, it is likely that the OH yield does peak at propene. A longer carbon chain also seems to reduce the OH yield for the branched alkenes. The difference for the 1-butene through 1-octene series and the branched alkenes may arise from the unknown amount of HO_2 that forms; the cyclohexane method is sensitive to HO_2 formation due to a competition between (R15a) and (R15b−d). It should be noted that formation of OH from HO_2 + O_3 is likely to be very small with either method. The cyclohexane method is based on a typical yield of those cyclohexane/cyclohexanol from reacted cyclohexane (55%, derived from α-pinene and Δ^3-carene measurements[8]). Recognition that this yield will change if the ratios of HO_2/RO_2 and $RO_2/C_6H_6O_2$ change is the source of the uncertainty attached

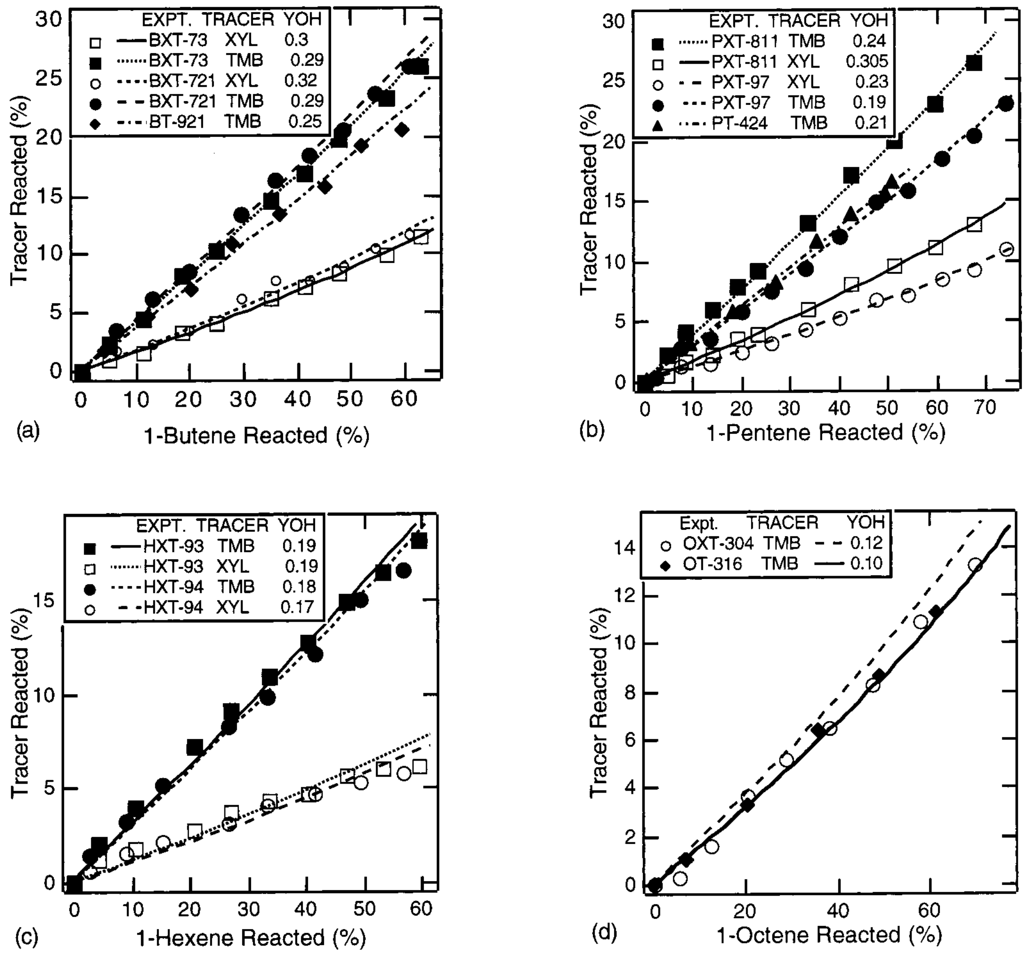

Figure 2. Data (symbols) and model calculations (lines) for representative 1-alkene experiments: (a) 1-butene; (b) 1-pentene; (c) 1-hexene; (d) 1-octene. Tracers and corresponding OH yields assumed in the calculations are indicated in the legends. In BT-921, a larger amount of tracer was added, thus the slope is lower than that for the other TMB experiments.

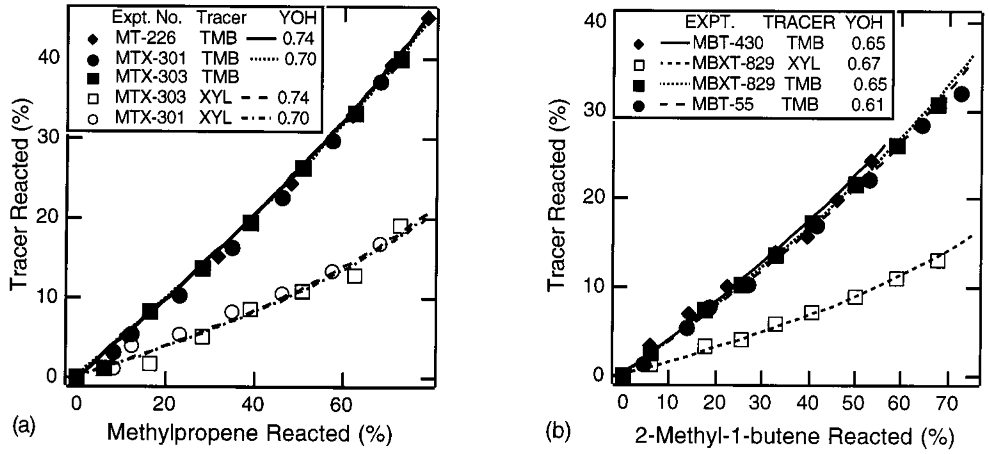

Figure 3. Data (symbols) and model calculations (lines) for representative methylpropene and 2-methyl-1-butene experiments: (a) methylpropene; (b) 2-methyl-1-butene. Tracers and corresponding OH yields assumed in the calculations are indicated in the legends.

by Atkinson and co-workers.[8,10] Clearly one explanation for the cyclohexane method resulting in a higher OH yield is for the HO_2 yield to be lower than typical.

The yield of propanal from the O_3−1-butene reaction was determined to be 0.45 ± 0.02 using cyclohexane as the scavenger (Table 2, Figure 5). The propanal yield measured here is significantly higher than that determined by Grosjean et al.[40] (0.35 ± 0.018) but is more in line with other terminal alkenes, which report yields of both formaldehyde and the corresponding $>C_1$ aldehyde to be roughly 0.5.

Mechanistic Implications

Figure 6 shows OH yields for several alkenes plotted as a function of the number of carbon atoms. Each olefin can nominally form four different carbonyl oxides (syn and anti from both sides of the double bond); this number is obviously decreased as the symmetry about the double bond increases. The number of possible syn and anti carbonyl oxides, coupled with the assumption that syn carbonyl oxides make OH with unit efficiently while the anti carbonyl oxides do not generate

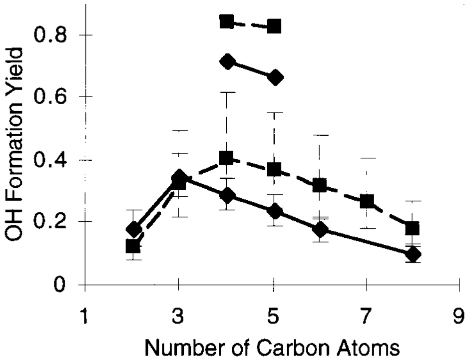

Figure 4. The OH formation yields for O_3 reaction with terminal alkenes as a function of the number of carbon atoms measured by this laboratory (diamonds, solid line) and by Atkinson and co-workers[10,38] (dashed line, squares). The lower series is ethene through 1-octene, and the upper pair is methylpropene and 2-methyl-1-butene.

appreciable OH, captures the broad features of OH formation, predicting the OH yield to within about 0.25 OH per olefin reacted. All four of the carbonyl oxides from 2,3-dimethyl-2-butene and 1,2-dimethylcyclohexene have an abstractable β-hydrogen atom, thus an OH yield in the neighborhood of 100% is anticipated; this is roughly what is observed (yOH = 70−100%, Table 1). Likewise, this simple model predicts an OH yield of about 75% from 2-methyl-2-butene (yOH = 93%), 50% from *cis*- and *trans*-2-butene (yOH = 64% and 37%, respectively), 50% from the cycloalkenes, and so forth (yOH = 62% to 34%, respectively). The terminal alkenes are complicated by the C_1 carbonyl oxide, which forms some OH but by a different mechanism than the syn carbonyl oxide. Propene (yOH = 35%) might be expected to produce about 34% OH, 25% from the *syn*-acetaldehyde oxide and 9% from the C_1 carbonyl oxide, half that of ethene.

While the number of possible syn and anti carbonyl oxides is clearly important to the OH formation yield, the fractional yields of the different carbonyl oxides, resulting from differences in the cycloreversion transition states,[42,43] also plays a role. The aldehyde coproducts provide insight into the preferences for different carbonyl oxides. For unbranched alkenes, both possible aldehydes have yields of about 50%; branched alkenes appear to favor formation of the substituted carbonyl oxide and formaldehyde in a ratio of about 70:30.[36,39] Thus, we expect that the OH formation yield from methylpropene (yOH = 72%) will be 55−70% from the acetone carbonyl oxide, plus a small amount from the C_1 fragment, in excellent agreement with the observed OH yield. 2-methyl-2-butene, 1-methylcyclohexene, and 2-methyl-1-butene (yOH = 0.93, 0.91, 0.67, respectively) all fit this model as well. *cis*- and *trans*-2-butene obviously generate only acetaldehyde; however, ab initio calculations coupled with measurements of the stereoisomers of the carbonyl oxide−aldehyde addition product in some solvents[71,72] suggests that *cis*-2-butene may generate more anti carbonyl oxide than trans. Thus, while the simplest model predicts 50% for both, this refinement adjusts the OH yield for cis down, and depending on the calculation, trans- up,[42,48] qualitatively explaining the higher OH yield from *trans*-2-butene (0.64, 0.54, 0.65[10,56,73]) compared to *cis*-2-butene (0.41, 0.33, 0.37,[10,56,73]). The combination of the number of possible *syn*-carbonyl oxides and the unequal breaking of asymmetric alkenes successfully predicts the OH yields within 0.1 or better per alkene reacted for the simplest alkenes of each type, but again, this depends on the tenuous assumption that syn and anti carbonyl oxides produce OH with unit and zero yield, respectively.

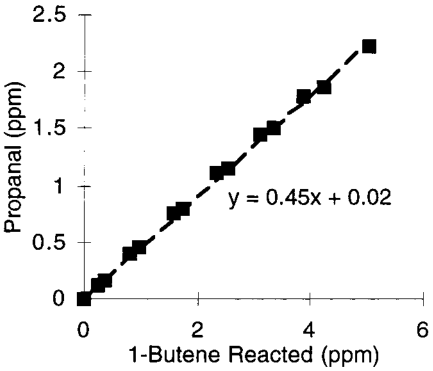

Figure 5. Propanal formation from the O_3 reaction with 1-butene using cyclohexane as a scavenger.

Certainly a striking feature of Figure 6 is the decreasing OH yields with increasing size for the terminal and cycloalkenes. This trend may not be duplicated beyond the C_4-C_5 boundary for the trans internal alkenes and not at all for the cis series.[73] A second striking feature of Figure 6 is the large jump in OH formation from the acyclic to cycloalkenes; for example, cyclopentene (yOH = 0.62) is double that of *cis*-2-pentene (yOH = 0.3), and cyclohexene is also higher. On the other hand, cycloheptene is in line with *cis*-2-butene and *cis*-3-hexene.

It is interesting to consider the relationship between the thermalized Criegee intermediate yield (summarized in Table 1, defined as a species that is long enough lived to undergo a secondary reaction, presumably a carbonyl oxide) and the OH formation yield, plotted in Figure 7. Most of the values are from Hatakeyama et al.,[74] because this is the largest data set and presumably has reasonable internal consistency; exceptions are noted. A correlation is given for the open symbols; the outliers, ethene and the (unsubstituted, endo) cycloalkenes, were not included. The outliers may be rationalized. Ethene is a special case with a different OH formation pathway, and the thermalized carbonyl oxides from the cycloalkenes might form an unreactive internal secondary ozonide.[74] It is not clear, however, why the methyl-substituted endocyclic compounds 1-methylcyclohexene and α-pinene have higher thermalized yields. It is worth noting that, unlike the OH yields, the thermalized carbonyl oxide yields have almost no dependence on the size of the molecule; for the most part the same type of bond has about the same thermalized Criegee intermediate yield. The thermalized Criegee intermediate and OH yields must be somewhat correlated since both are significant pathways and the total yield is limited. The fact that the correlation is far from 1:1 does not seem to imply a tight mechanistic coupling.

The tendency for OH formation to decrease for increasing carbon backbones obviously suggests a collisional stabilization process is important. In another study, we have investigated the pressure dependence of the OH yields and find that, within uncertainties, the OH yields are pressure dependent only for ethene and propene and not for *trans*-2-butene, 1-butene, 2,3-dimethyl-2-butene, cyclopentene, or *trans*-3-hexene over the range 20−760 Torr and at higher effective pressures with added SF_6.[48] An alternate, more detailed explanation for the possible source of pressure dependence for ethene and propene will be discussed elsewhere.[48] Both the lack of pressure dependence of the OH yield and its equivocal relationship between the thermalized carbonyl oxide yields indicates that collisional stabilization is not likely to explain the higher yields from cycloalkenes or the trend to decreasing OH with longer chain length for the 1-alkenes.

In another study, we have investigated OH formation from cycloalkenes.[43] Theoretical calculations indicate that the trends

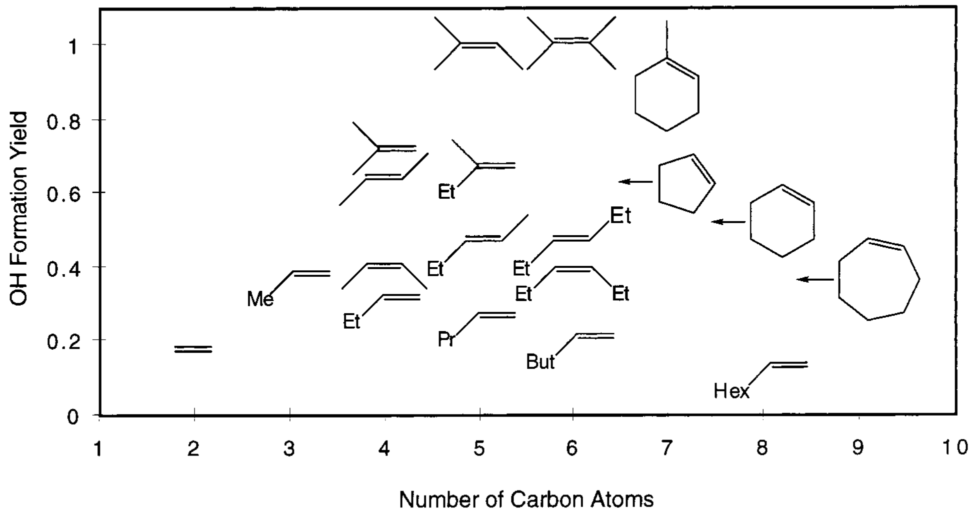

Figure 6. The formation of OH radicals as a function of the number of carbon atoms in the reacting alkene. The cycloalkenes are shifted with respect to the abscissa by two carbons to relieve congestion in the plot.

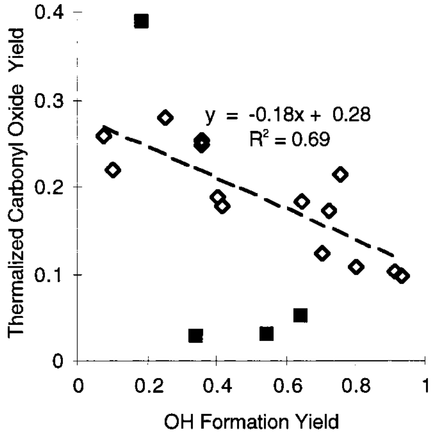

Figure 7. Relationship between the thermalized carbonyl oxide yield and the OH formation yield (Table 1). The correlation shown includes only the open symbols. The outliers (solid squares) are ethene (above) and cyclopentene, cyclohexene, and cycloheptene (below).

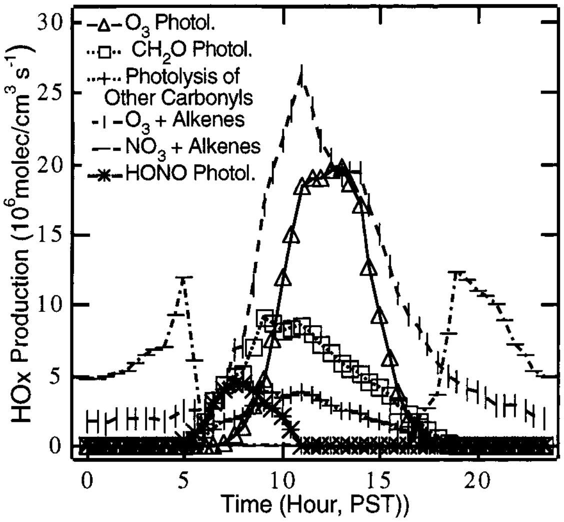

Figure 8. HO_x formation rates for an average of two moderately polluted Los Angeles stations, using an average speciated mix for VOC's and hourly NMHC, O_3, and NO_x measurements. Reprinted with permission from ref 14.

for these compounds, as well as their high yields compared to the acyclic compounds, can be explained by the energies of the cycloreversion transition states, constrained by the preferred conformations of the five-, six-, and seven-membered rings.[43]

The OH yield trends for terminal alkenes remain to be explained. We offer two possibilities: First, there may be a kinetic competition between the isomerization reactions and the rate of intramolecular vibrational energy redistribution (IVR). In this hypothesis, for large carbonyl oxides, the excess vibrational energy spreads into vibrational modes away from the carbonyl oxide moiety sufficiently rapidly to reduce OH formation (R3a), predicting a process that is independent of pressure if OH formation from the vibrationally "relaxed" carbonyl oxide is small. While processes that can compete with IVR are unusual, Olzmann et al.[49] used ab initio/RRKM calculations to predict the rates of OH formation from ethene and 2,3-dimethyl-2-butene, finding time scales of 10^{-9}–10^{-11} seconds. Alternatively, the energy of the carbonyl oxides may change such that OH from the C_1, anti or to a lesser degree the syn carbonyl oxide is decreased as the carbon chain length increases. The energy partitioning in the decomposing primary ozonide will depend somewhat on the number of available vibrational modes, which increases rapidly as carbon atoms are added to the molecule. Clearly more theoretical work is needed to determine the source of these behaviors. More experimental work is also needed to resolve some of the discrepancies discussed here, as well as the many related issues not included in this contribution.

Atmospheric Implications: HO_x Production in Urban and Rural Air

Figure 8 (redrawn from ref 14) shows the diurnal variation of HO_x (HO_x = OH, HO_2, and RO_2) radical sources in Los Angeles, including the contribution from O_3–alkene reactions. This calculation assumed a total HO_x yield from alkene ozonolysis that was double the measured OH yield due to the RO_2 radical that is coproduced with OH (R3a) and is generally converted to HO_2 in the atmosphere via (R5).[14] In the early morning, before O_3 builds up (or is transported down from aloft), photolysis of carbonyls and HONO dominates radical production. After about 8:00 AM, the reaction of O_3 with alkenes is the largest single HO_x source, and it is especially significant after about 4:00 PM when the O_3 levels are still high and photolysis has slowed. During the night, NO_3 reactions with alkenes are the dominant HO_x source. However, the importance of this source may have been significantly overestimated, since

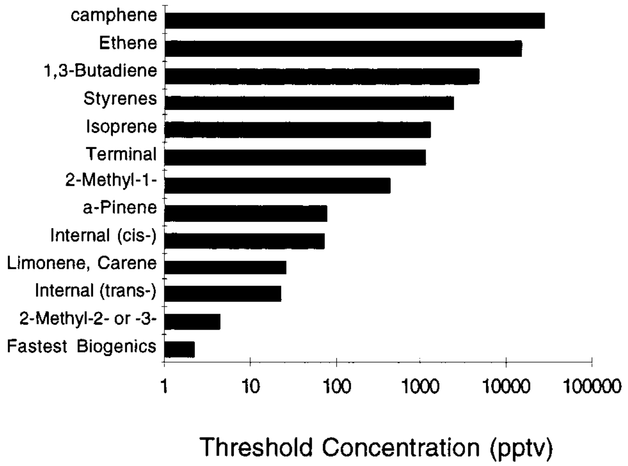

Figure 9. Threshold concentrations for several anthropogenic and biogenic alkenes. At these ambient concentrations, the reaction between an alkene and O_3 could be expected to contribute about 1% at noon or 2−3% over the course of 24 h to primary HO_x production in urban air.

rapid interconversion between RO_2, HO_2, and OH does not take place without NO and very low levels of NO are often observed to accompany higher concentrations of NO_3.[75] A detailed breakdown of the contributions to HO_x production from the alkene mix assumed for Figure 8 indicates that the most active alkenes are species present at low concentration, in particular the internal alkenes. For example, the top four contributors are *trans*-2-butene, 2-methyl-2-pentene, and *cis*- and *trans*-2-pentene. These account for 72% of the HO_x from alkenes yet are only 5% of the total alkenes, and less than 2% of the total VOC's (on a carbon basis). Calculations of HO_x production for many other cities based on measured data sets[3,5] show that internal alkenes are typically dominant contributors. By contrast, ethene and propene, which are commonly included in the chemistry module of airshed models,[16−18] account for less than 10% of the new HO_x arising from O_3−alkene reactions. Radical formation from internal alkenes is high, but more importantly, internal alkenes react more rapidly (by a factor of 10 or more) with O_3 than do terminal alkenes.

In Figure 9, we show approximate "threshold" concentrations for a number of alkenes, concentration levels above which the O_3 reactions could be expected to have a nonnegligible contribution to primary HO_x production in urban air. The calculations assumed that a given alkene reacting with 100 ppb of O_3 would account for production of about 1% of HO_x radicals at solar noon, 34° N latitude (and total aldehyde concentration of about 5 ppb, half of which was formaldehyde). Since photolysis of O_3 and aldehydes is highest at noon, the contribution from O_3−alkene reactions is minimized, and this level of HO_x production might translate into a 2−3% contribution per olefin over a 24 h period. It should be noted that the contribution of the O_3−alkene reaction vs O_3 photolysis does not depend on the O_3 concentration but rather the solar flux and the alkene concentrations. Straight chain terminal alkenes react slowly with O_3 and produce moderate amounts of OH and RO_2 radicals, thus their "thresholds" are a few ppb. The "thresholds" for the internal alkenes are quite low, 10−100 ppt. Each of these compounds is commonly observed above these "thresholds".[1−3,5] Compounds with more than seven carbons and internal double bonds may be present at above the "threshold" concentrations, but they are typically not included in ambient air analyses.

A similar calculation to the urban air case was performed for rural air[14] observed in the southeastern United States.[76] The most important biogenic species in terms of radical production were isoprene (6.3 ppbv average daytime mixing ratio) and α-pinene (0.3 ppbv), with approximately equal contributions from each. Over a full diurnal cycle, O_3−alkene reactions account for 20−25% of total HO_x. The importance of the O_3−alkene reactions is greatest in the late afternoon and early evening due to the enhanced O_3 levels and slowed photolysis rates at these times, and these reactions become the dominant single source of radicals after about 5:00 PM.

Recently, a handful of field investigations[15,77] and more complete modeling studies have addressed the importance of alkene−O_3 reactions. Making a complete assessment with field measurements and modeling is an ambitious task since it is best performed with a large data set that includes measurement data for several HO_x precursors, meteorological data, difficult measurements of OH, HO_2, and RO_2, and an up to date model of chemistry and physics. In 1995, Hu and Stedman[15] made measurements of RO_2 in Denver, CO and found that alkene ozonolysis was needed to explain the observed levels of RO_x, especially in the evening. Recently, George et al.[77] made measurements of OH and HO_2 in Los Angeles, CA. They modeled these measurements together with hydrocarbon and inorganic data with chemistry from Lurmann et al.[16] and found the model RO_x levels to be higher than the measured levels. The Lurmann et al.[16] chemistry contains roughly 10% of the HO_x source from alkene ozonolysis, together with other chemistry reflecting the understanding of a dozen years ago. Bey et al.[78] modeled the nocturnal stable layer in rural and urban air with current NO_3− and O_3−alkene chemistry and found that particularly the latter reaction leads to nighttime OH concentrations in urban air of $(1-8) \times 10^5$ molec^{-1} cm^3. Their calculated range for OH in rural air was 3×10^4 to 2×10^5 molec^{-1} cm^3,[78] consistent with several observations of OH, RO_2, and HO_2.[79,80]

In rural areas, a rapid loss of isoprene in the evening in forests has been observed in several locations including Alabama, Michigan, and Ontario.[76,81,82] The isoprene decay does not appear to be attributable to mixing or other usual loss processes,[76,81] and it is likely that O_3−alkene reactions can explain at least some of the "missing sink".[14] The recent study by Makar et al.[81] modeling data from an Ontario diciduous forest corroborates this hypothesis, even though the chemistry they used to analyze the observations included OH yields that were about half the measured values.

Conclusions

A growing data set has established that OH formation is a major pathway for the reaction of alkenes with O_3 and OH is produced with efficiency of 7−100%[10,28,29,56] The broad features of the relationship between alkene structure and OH yields can be explained by the formation and expected quantities of syn and anti carbonyl oxides, coupled with the assumption that OH formation from syn approaches unity while OH formation from anti is small. Sufficient data now exists (or will soon) to make reasonable predictions for OH yields based on similar structures. Within the general framework, however, several issues remain unsloved. The formation and pressure dependence of OH from ethene has not been satisfactorily explained, and other special cases such as styrene and some of the oxygenated alkenes still need consideration. The decreasing OH yields from the terminal and cyclic alkene series coupled with a lack of a pressure dependence and lack of a strong (inverse) relationship with the yield of thermalized carbonyl oxides is difficult to rationalize. In addition to verification of the pressure dependence behavior, ab initio, RRKM, and related theoretical investigations would be most useful. An absolute rate constant for a reaction of a thermalized carbonyl oxide has yet to be measured, and, still, a spectroscopic identification of a thermalized (or other) carbonyl oxide would obviously be enlightening. For application to the atmosphere, an investigation (while difficult) of an O_3−alkene reaction in the presence of NO may prove valuable. While the contribution to HO_x formation in the atmosphere is clearly significant under many conditions, the impact of these reactions in the field has yet to be thoroughly investigated.

Acknowledgment. Acknowledgment is made to the National Science Foundation, ATM-9629577, and the Environmental Protection Agency. Assistance with some experiments was provided by Ping Liu and Dr. Atish Sen. We thank Prof. K. N. Houk, Dr. K. K. Kuwata, and J.D. Fenske for helpful discussions and Dr. G. Marston, A.R. Rickard, D. Johnson, and Dr. C. D. McGill for sharing their data prior to publication. Finally, we acknowledge the careful work and helpful suggestions of two anonymous reviewers.

References and Notes

(1) Fraser, M. P.; Cass, G. R.; Simonet, B. R. T.; Rasmussen, R. A. *Environ. Sci. Technol.* **1997**, *31*, 2356−2367.

(2) Seinfeld, J. H. In *Current Problems and Progress in Atmospheric Chemistry*; Barker, J., Ed.; World Scientific Publishing Co.: River Edge, NJ, 1996; p 34−57.

(3) Blake, N. J.; Penkett, S. A.; Clemitshaw, K. C.; Anwyl, P.; Lightman, P.; Marsh, A. R. W.; Butcher, G. *J. Geophys. Res.* **1993**, *98*, 2851−2864.

(4) Zielinska, B.; Sagebiel, J. C.; Harshfield, G.; Gertler, A. W.; Pierson, W. R. *Atmos. Environ.* **1996**, *30*, 2269−2286.

(5) Jeffries, H. E. In *Composition, Chemistry and Climate of the Atmosphere*; Singh, H. B., Ed.; Van Nostrom Reinhold: New York, 1995.

(6) Hatakeyama, S.; Akimoto, H. *Res. Chem. Intermed.* **1994**, *20*, 503−524.

(7) Niki, H.; Maker, P. D.; Savage, C. M.; Breitenbach, L. P.; Hurley, M. D. *J. Am. Chem. Soc.* **1987**, *91*, 941−946.

(8) Atkinson, R.; Aschmann, S. M.; Arey, J.; Shorees, B. *J. Geophys. Res.* **1992**, *97*, 6065−6073.

(9) Paulson, S. E.; Flagan, R. C.; Seinfeld, J. H. *Int. J. Chem. Kinet.* **1992**, *24*, 79−102.

(10) Atkinson, R.; Aschmann, S. M. *Environ. Sci. Technol.* **1993**, *27*, 1357−1363.

(11) Paulson, S. E.; Sen, A. D.; Liu, P.; Fenske, J. D.; Fox, M. J. *Geophys. Res. Lett.* **1997**, *24*, 3193−3196.

(12) Donahue, N. M.; Kroll, J. H.; Anderson, J. G.; Demerjian, K. L. *Geophys. Res. Lett.* **1998**, *25*, 59−62.

(13) Gutbrod, R.; Kraka, E.; Schindler, R. N.; Cremer, D. *J. Am. Chem. Soc.* **1997**, *119*, 7330−7342.

(14) Paulson, S. E.; Orlando, J. J. *Geophys. Res. Lett.* **1996**, *23*, 3727−3730.

(15) Hu, J.; Stedman, D. H. *Environ. Sci. Technol.* **1995**, *29*, 1655−1659.

(16) Lurmann, F. W.; Carter, W. P. L.; Coyner, L. A. Report No. EPA/600/3-87/014; Environmental Protection Agency, 1987.

(17) McKeen, S. A.; Hsie, E.-Y.; Trainer, M.; Tallamraju, R.; Liu, S. C. *J. Geophys. Res.* **1991**, *96*, 10809−10845.

(18) Gery, M. W.; Whitten, G. Z.; Killus, J. P.; Dodge, M. C. *J. Geophys. Res.* **1989**, *94*, 12925−12956.

(19) Saltzmann, B. E. *Ind. Eng. Chem.* **1958**, *50*, 677.

(20) Nederbragt, G. W.; vanderHorst, A.; vanDuijn, J. *Nature* **1965**, *4979*, 87.

(21) Kummer, W. A.; Pitts, J. J. N.; Steer, R. P. *Environ. Sci. Technol.* **1971**, *5*, 1045−1048.

(22) Finlayson, B. J.; Pitts, J. J. N.; Akimoto, H. *Chem. Phys. Lett.* **1972**, *12*, 495−500.

(23) Atkinson, R.; Finlayson, B. J.; Pitts, J. J. N. *J. Am. Chem. Soc.* **1973**, *95*, 7592−7599.

(24) Martinez, R. I.; Herron, J. T.; Huie, R. E. *J. Am. Chem. Soc.* **1981**, *103*, 3807−3820.

(25) Paulson, S. E.; Flagan, R. C.; Seinfeld, J. H. *Int. J. Chem. Kinet.* **1992**, *24*, 103−125.

(26) Paulson, S. E.; Seinfeld, J. H. *Environ. Sci. Technol.* **1992**, *26*, 1165−1173.

(27) Chew, A. A.; Atkinson, R. *J. Geophys. Res.* **1996**, *101*, 28649−28653.

(28) Gutbrod, R.; Meyer, S.; Rahman, M. M.; Schindler, R. N. *Int. J. Chem. Kinet.* **1997**, *29*, 717−723.

(29) Paulson, S.; Chung, M.; Sen, A.; Orzechowska, G. *J. Geophys. Res.* **1998**, *103*, 25533−25539.

(30) Marston, G.; McGill, C. D.; Rickard, A. R. *Geophys. Res. Lett.* **1998**, *25*, 2177−2180.

(31) Paulson, S. E.; Fenske, J. D.; Sen, A.; Callahan, T. W. *J. Phys. Chem. A* **1999**, *103*, 2050−2059.

(32) Criegee, R.; Wenner, G. *Liebigs Ann. Chem.* **1949**, *564*, 9.

(33) Criegee, R. *Angew. Chem. Int. Ed.* **1975**, *14*, 745−752.

(34) Atkinson, R.; Aschmann, S. M.; Arey, J.; Tuazon, E. C. *Int. J. Chem. Kinet.* **1994**, *26*, 945−950.

(35) Kramp, F.; Paulson, S. E. *Atmos. Environ.*, in press.

(36) Grosjean, E.; Grosjean, D. *Environ. Sci. Technol.* **1997**, *31*, 2421−2427.

(37) Tuazon, E. C.; Aschmann, S. M.; Arey, J.; Atkinson, R. *Environ. Sci. Technol.* **1997**, *31*, 3004−3009.

(38) Atkinson, R.; Tuazon, E. C.; Aschmann, S. M. *Environ. Sci. Technol.* **1995**, *29*, 1860−1866.

(39) Atkinson, R. *J. Phys. Chem. Ref. Data* **1997**, *26*, 215−290.

(40) Grosjean, E.; deAndrade, J. B.; Grosjean, D. *Environ. Sci. Technol.* **1996**, *30*, 975−981.

(41) Hakola, H.; Arey, J.; Aschmann, S. M.; Atkinson, R. *J. Atmos. Chem.* **1994**, *18*, 75−102.

(42) Rathman, W. D.; Claxton, T. A.; Rickard, A. R.; Marston, G. *Phys. Chem. Chem. Phys.*, in press.

(43) Fenske, J. D.; Kuwata, K. T.; Houk, K. N.; Paulson, S. E., 1999. Unpublished work.

(44) Bunnelle, W. M. *Chem. Rev.* **1991**, *91*, 335−362.

(45) Gutbrod, R.; Schindler, R. N.; Kraka, E.; Cremer, D. *Chem. Phys. Lett.* **1996**, *252*, 221−229.

(46) Bach, R.; Owensby, A.; Andres, J.; Schlegel, H. *J. Am. Chem. Soc.* **1992**, *114*, 7207−7217.

(47) Anglada, J. M.; Bofill, J. M.; Olivella, S.; Sole, A. *J. Am. Chem. Soc.* **1996**, *118*, 4636−4647.

(48) Fenske, J. D.; Kuwata, K. T.; Hasson, A. S.; Ho, A. W.; Houk, K. N.; Paulson, S. E., 1999. Unpublished work.

(49) Olzmann, M.; Kraka, E.; Cremer, D.; Gutbrod, R.; Schindler, R. *J. Phys. Chem. A* **1997**, *101*, 9421−9429.

(50) Horie, O.; Neeb, P.; Moortgat, G. K. *Int. J. Chem. Kinet.* **1994**, *26*, 1075−1094.

(51) Pfeiffer, T.; Forberich, O.; Comes, F. J. *Chem. Phys. Lett.* **1998**, *298*, 351−358.

(52) Schafer, C.; Horie, O.; Crowley, J. N.; Moortgat, G. K. *Geophys. Res. Lett.* **1997**, *24*, 1611−1614.

(53) McGill, C.; Rickard, A.; Johnson, D.; Marston, G. *Chemosphere* **1999**, *38*, 1205−1212.

(54) Shu, Y.; Atkinson, R. *Int. J. Chem. Kinet.* **1994**, *26*, 1193−1205.

(55) Alvarado, A.; Tuazon, E. C.; Aschmann, S. M.; Arey, J.; Atkinson, R. *Atmos. Environ.* **1999**, *33*, 2893−2905.

(56) Rickard, A. R.; Johnson, D.; McGill, C. D.; Marston, G. *J. Phys. Chem.*, in press.

(57) Horie, O.; Moortgat, G. K. *Chem. Phys. Lett.* **1998**, *288*, 464−472.

(58) Atkinson, R. *J. Phys. Chem. Ref. Data* **1994**, Monograph no. 2, 1−216.

(59) Finlayson-Pitts, B. J.; Pitts, J. *Atmospheric Chemistry: Fundamentals and Experimental Techniques*; New York: Wiley-Interscience, 1986.

(60) Taylor, J. R. *An Introduction to Error Analysis*, 1st ed.; University Science Books: Mill Valley, CA, 1982.

(61) Kramp, F.; Paulson, S. E. *J. Phys. Chem.* **1998**, *102*, 2685−2690.

(62) Neeb, P.; Horie, O.; Moortgat, G. K. *Int. J. Chem. Kinet.* **1996**, *28*, 721−730.

(63) Mihelcic, D.; Heitlinger, M.; Kley, D.; Musgen, P.; Volz-Thomas, A. *Chem. Phys. Lett.* **1999**, *301*, 559−564.

(64) Suenram, F. J.; Lovas, F. J. *J. Am. Chem. Soc.* **1978**, *100*, 5117−5122.

(65) Horie, O.; Moortgat, G. K. *Atmos. Environ.* **1991**, *25A*, 1881−1896.

(66) Thamm, J.; Wolff, S.; Turner, W.; Gab, S. *Chem. Phys. Lett.* **1996**, *258*, 155−158.

(67) Jorgensen, A. D.; Picel, K. C.; Stamoudis, V. C. *Anal. Chem.* **1990**, *62*, 683−689.

(68) Orlando, J. J.; Tyndall, G. S.; Noziere, B.; Orzechowska, G.; Paulson, S. E.; Rudich, Y. Unpublished work.

(69) Paulson, S. E.; Meller, R.; Chung, M. Report no. 95-335; California Air Resources Board, 1999.

(70) Lightfoot, P. D.; Cox, R. A.; Crowley, J. N.; Destriau, M.; Hayman, G. D.; Jenkin, M. E.; Moortgat, G. K.; Zabel, F. *Atmos. Environ.* **1992**, *26A*, 1805−1961.

(71) Bailey, P. S.; Ward, J. W.; Carter, J. T. P.; Nieh, E.; Fischer, C. M.; Khashab, A. Y. *J. Am. Chem. Soc.* **1974**, *96*, 6136−6140.

(72) Cremer, D. *J. Am. Chem. Soc.* **1981**, *103*, 3627−3633.

(73) Orzechowska, G.; Paulson, S. E., 1999. Unpublished work.

(74) Hatakeyama, S.; Kobayashi, H.; Akimoto, H. *J. Phys. Chem.* **1984**, *88*, 4736−4739.

(75) Mackay, G. I. Report no. A92-327; California Air Resources Board, 1994.

(76) Goldan, P. D.; Kuster, W. C.; Fehsenfeld, F. C. *J. Geophys. Res.* **1995**, *100*, 25945−25963.

(77) George, L. A.; Hard, T. M.; O'Brian, R. J. *J. Geophys. Res.* **1999**, *104*, 11643−11655.

(78) Bey, I.; Aumont, B.; Toupace, G. *Geophys. Res. Lett.* **1997**, *24*, 1067−1070.

(79) Tanner, D. J.; Eisele, F. L. *J. Geophys. Res.* **1995**, *100*, 2883−2892.

(80) Mihelcic, D.; Klemp, D.; Musgen, P.; Patz, H. W.; Volz-Thomas, J. *J. Atmos. Chem.* **1993**, *16*, 313−335.

(81) Makar, P. A.; Fuentes, J. D.; Wang, D.; Staebler, R. M.; Wiebe, H. A. *J. Geophys. Res.* **1999**, *104*, 3581−3603.

(82) Herrera-Gomez, O.; Splawn, B. G.; Shepson, P. B.; Hastie, D. R.; Mihele, C.; Carroll, M. A.; Thornberry, T.; Emmons, L. K.; Bertmann, S. B. *American Geophysical Union Spring Meeting*, Boston, MA, 1998.

(83) Atkinson, R.; Arey, J.; Aschmann, S. M.; Corchnoy, S. B. *Int. J. Chem. Kinet.* **1995**, *10*, 941−955.